Key Engineering Materials
ISSN: 1662-9795, Vol. 964, pp 59-64
doi:10.4028/p-rl51NI

Submitted: 2023-05-23
Accepted: 2023-09-12
Online: 2023-11-23

Process Parameter Prediction in Laser Powder Bed Fusion Using an Artificial Neural Network

Natan Nudelis[1,2,a*], Peter Mayr[2,b]

[1]FIT AG, 92331 Lupburg, Germany

[2]TUM School of Engineering and Design, Department of Mechanical Engineering, Chair of Materials Engineering of Additive Manufacturing, Technical University of Munich, 85748 Garching, Germany

[a]natan.nudelis@pro-fit.de, [b]peter.mayr@tum.de

Keywords: Laser powder bed fusion, AlSi10Mg, Computed tomography, Pore classification, Artificial neural network

Abstract. Pores are the inevitable concomitant in the current state of laser powder bed fusion (PBF-LB/M) of AlSI10Mg components. Various pore characteristics, such as pore size and pore shape, influence the quality and affect the intended functionality of the component. Today, the experimental effort to find the appropriate process parameters for additive manufacturing (AM) results in high costs and long time-to-market. Pore formation is highly dependent on the applied process parameters. Consequently, pores can also be seen as an individual process fingerprint. Computed tomography is a commonly used measurement tool for AM components and can be used to comprehensively investigate process-induced defects. Furthermore, X-ray data allows an accurate categorisation of pores and provides a large amount of labelled data for supervised learning applications. The applied classification method classifies the pores into six classes (A-F) according to their shape and size. A total number of 3,066,249 pores detected in cylindrical samples were categorised and used for machine learning. The purpose of this work is to demonstrate an approach for predicting AM process parameters depending on the resulting pore distribution using supervised learning methods. The result is an expandable machine learning model based on an artificial neural network.

Introduction

Previous studies have focused extensively on investigating the types and origins of pores in the PBF-LB/M process [1-6]. However, porosity remains a common by-product of laser powder bed fusion of Al alloys. Three types of pores have been identified as the most common, which can be categorised into spherical and irregularly shaped classes. Spherical pores are recognised as either hydrogen-induced or keyhole pores, while the so-called lack of fusion porosity has a highly irregular shape. On the one hand, the formation of these types of pores can provide valuable insights into the process conditions and influence the mechanical properties of the final product. Several research reports have been published on process optimisation of the PBF-LB/M process using AlSi10Mg [2,4,7-10]. On the other hand, computed tomography appears to be a suitable technology for the collection of pore data, particularly in case of aluminium alloys. Many previous studies have demonstrated the accuracy of X-ray data for defect detection and pore distribution analysis [11-14]. For classification tasks, supervised machine learning offers a promising approach. The proposed method involves training a neural network with labelled pore data from the X-ray scans and process parameters. The goal is to predict process parameters based on the resulting pore distribution.

Methods

The cylindrical specimens, analysed in this study, were fabricated at FIT AG using the SLM500 PBF-LB/M machine (SLM Solutions, Lübeck, Germany). The machine is equipped with a Nd:YAG laser (λ = 1064 nm) that has a maximum laser output of 400 W, with the working point usually set at 350 W. All specimens were built using AlSi10Mg powder (Tekna Advanced Materials Inc., Sherbrooke, Canada). The specimen orientation was chosen to be vertical to the building platform.

The chemical composition of the powder used in this study can be seen exemplarily in Nudelis et al. [15]. A total of 32 PBF-LB/M parameter sets were evaluated to determine their impact on pore formation. The scanning speed v (1000 mm/s, 1250 mm/s, 1500 mm/s, 1750 mm/s), the hatch distance h (0.125 mm, 0.15 mm, 0.175mm, 0.2 mm) and the layer thickness t (30 µm, 40 µm, 60 µm, 80 µm) were varied. Finally, 3,066,249 pores from 96 cylindrical specimens formed the pore database. Each parameter set is represented by 3 specimens. These pores were then used to train the neural network. A simple cylindrical specimen geometry (10 mm diameter, 18 mm height) was chosen for the X-ray scans to facilitate consistent scanning with minimal CT-artifacts. A Diondo d2 microfocus CT-system (Hattingen, Germany) with a minimum voxel size of 9.659 µm³ was used for scanning. The specimen was rotated 360° in 1500 projections, with an integration time of 1.4 seconds per projection, using a power output of 9.5 W and a voltage of 190 kV. The raw CT data were reconstructed into a 3D model using VGSTUDIO MAX 3.1.0 64 by (Volume graphics, Heidelberg, Germany). Porosity analysis was carried out using the VGDefx algorithm, with a region of interest (ROI) of 785.4 mm³.

Table 1. Parameter sets for additional generalisation check

Parameter Set	Scanning Speed [mm/s]	Hatch Distance [mm]	Layer Thickness [µm]
1	1125	0.1275	35
2	1600	0.17	35
3	1400	0.155	70
4	1200	0.12	70
5	1700	0.19	70

The neural network approach was chosen in order to allow reliable process parameter or pore class prediction using supervised machine learning. The fully-connected neural network deals with a multi-class classification problem [16] for predicting pore types. All neurons within the hidden layers are connected with the log-sigmoid transfer function [17]. This ensures that there are no negative outputs, which are simply not present in this type of classification. Additionally, the log-sigmoid transfer function normalises the input to a finite range of positive values between 0 and 1. The log-sig function is also differentiable, which is essential for the multi-layer backpropagation network [17] used in this work. The output layer employs the softmax transfer function [17] to generate the final classification result. As input, the neural network takes the layer thickness (µm), the hatch distance (mm) and the scanning speed (mm/s). The output consists of the resulting pore classes A-F, as defined by the classification method in Nudelis et al. [18]. The optimal configuration of the neural network, including the number of layers and neurons per layer, is determined using the grid search technique [19]. The number of layers is varied incrementally from 1 to 5, while the number of neurons per layer ranges from 1 to 20. Finally, performance metrics such as Brier-score [20], the area under the ROC curve (AUC) [21] and cross-entropy are utilised to evaluate the neural network variants. Matlab R2021b (Natick, MA, USA) was used to create the neural network. The transfer, performance, training and initialisation functions are set as constant hyperparameters. The cross-entropy served as a performance function, while the scaled conjugate gradient backpropagation (trainscg) was used as the training function [22]. The networks are trained on the training data set (70 %) until the performance on the validation data set (15 %) starts to decrease, indicating that the generalisation ability of the network has reached its peak. Additionally, the test data set (15 %) is reserved for an independent assessment of the network's generalisation. The data are randomised before being split into training, validation and test data sets. The Nguyen-Widrow layer initialisation function (*initnw*) was used to initialise the weights and biases of the layer. This function is based on Nguyen et al. [23]. Due to the lack of data variation, an additional generalisation check on new data (5 unknown

parameter variations) is performed as well (Table 1). The average deviation (error) between these measured and predicted values must be as small as possible.

Results and Discussion

Hyperparameter optimisation was carried out to investigate the impact of varying the number of hidden layers (1-5) and neurons (1-20) on the performance of the network. Several performance metrics, including area under the ROC curve (AUC), the Brier-score and the cross-entropy were used to evaluate the network. All classification networks were successfully trained. The best fully-connected network consisted of 1 hidden layer and 9 neurons per layer and showed an AUC of 0.6280, a Brier-score of 0.1072 and cross-entropies of 0.1989 - 0.1992 for the training, test and validation sets. Further explanation of the meaning of the performance metrics can be found in [20-21]. The generalisation check reached an average deviation of 1.04 %. The designed neural network is capable of predicting several million combinations of process parameters based on the pore type distribution. The network was trained using typical parameter ranges for PBF-LB/M with AlSi10Mg (Fig. 1). These ranges were also used for the following parameter predictions. Assuming that the scanning speed can be set in 750 increments (ranging from 1000 mm/s to 1750 mm/s in 1 mm/s steps), the hatch distance in 300 increments (ranging from 0.125 mm to 0.2 mm in 0.00025 mm steps) and the layer thickness in 200 increments (ranging from 30 µm to 80 µm in 0.25 µm steps). This would result in 45,000,000 predictable parameter combinations, each with corresponding pore type distributions.

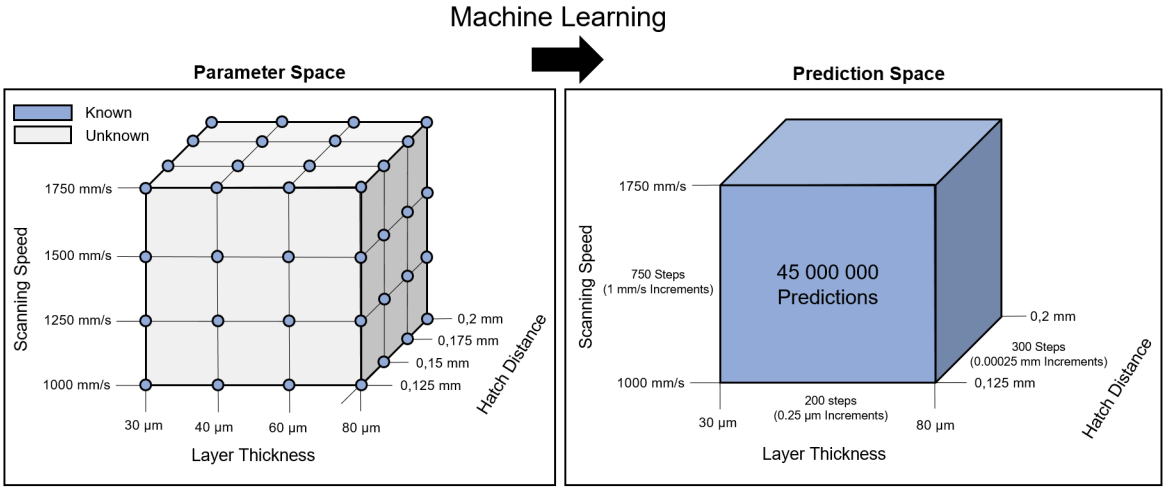

Fig. 1. Illustration of the initial parameter space and the prediction space after the machine learning process. Input values are the scanning speed, layer thickness and hatch distance. Output values are the pore types A-F.

It is obvious that not all of these combinations can be visualised, which is why the 5 unknown parameter cases from the generalisation check are used for the following prediction example. Figure 2 shows the predicted results, divided into 9 parameter cases, where only one parameter is varied while the others remain constant. The predictions follow the same trends as the measurements, which represent unknown data for the used network. Nevertheless, there may be discrepancies between the predictions and the real behaviour due to lack of data. Process parameters are undoubtedly crucial in the context of part quality [2,4,7,24]. However, several other influences contribute to the final part quality, including powder characteristics, machine equipment, finishing processes and part geometries [25]. This work only considers a limited number of process parameters. Additional inputs must be generated to improve the predictive capabilities. Further discrepancies may occur due to missing information. Any changes in powder characteristics, material or manufacturing technology may lead to deviations between predicted and actual results. The networks were trained solely on virgin AlSi10Mg powder from the same supplier, processed using SLM500 machines. Moreover,

predictions closer to known parameter data sets or industrial conditions are expected to yield better results than those in completely unknown parameter ranges.

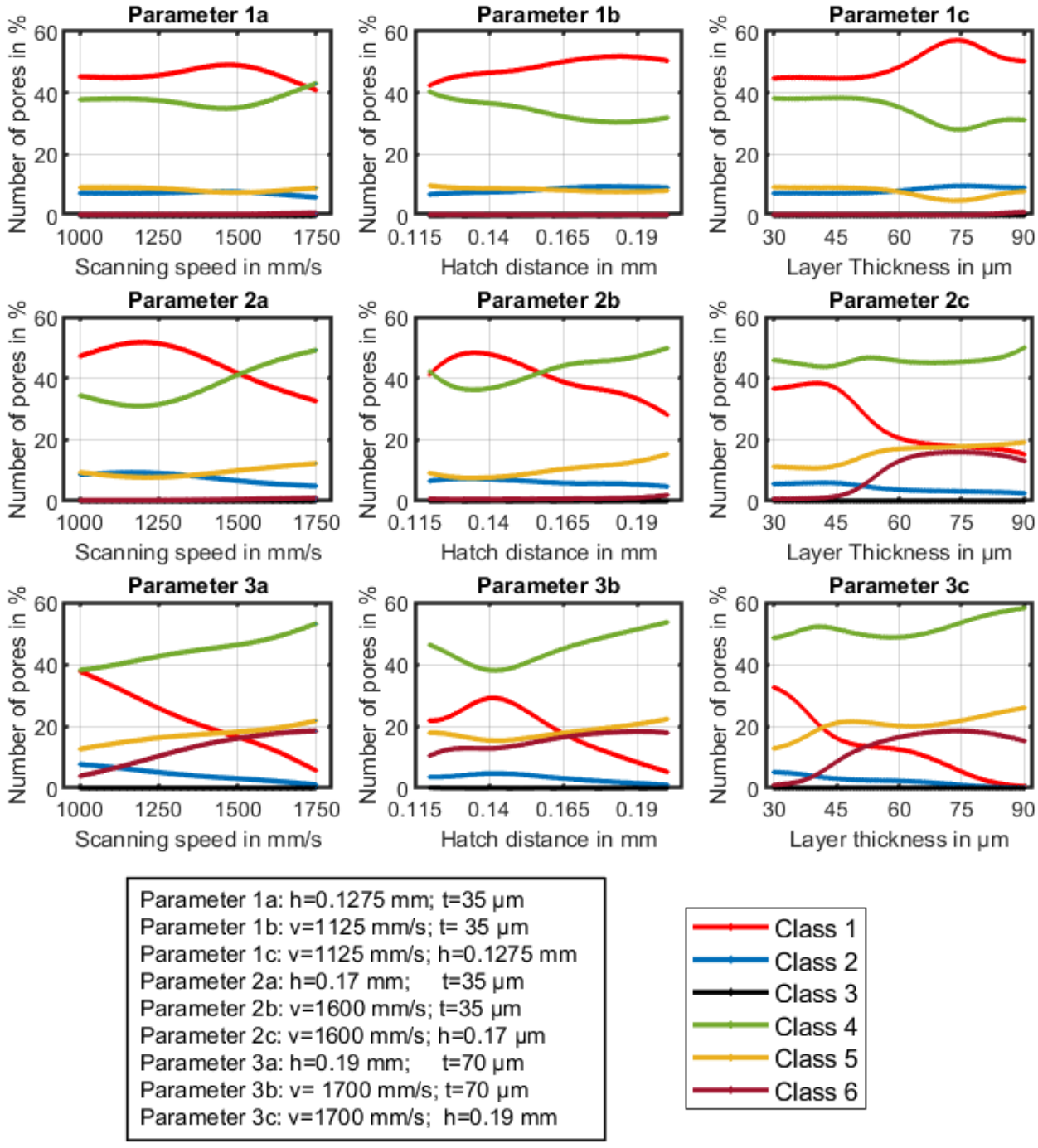

Fig. 2. Pore class prediction of 9 parameter cases (varied scanning speeds (v), hatch distances(h) and layer thicknesses (t))

Conclusion

Additive manufacturing is recognised for its design freedom, flexibility and numerous other benefits [26-27]. However, challenges related to reproducibility and functionality still limit the potential of AM and hinder its widespread adoption in many industries. Supervised machine learning can help to overcome quality constraints, reduce costs and time-to-market. The developed machine-learning based prediction model offers a flexible and cost-effective solution for customised AM-projects.

Nevertheless, further research should expand the current models to include a greater number of parameter variations, as well as other significant influencing factors such as powder characteristics, other manufacturing technologies and materials and additional human or process-related influences. A greater number and variety of data will lead to better generalisation and reduce the number of incorrect predictions.

References

[1] C. Weingarten, D. Buchbinder, N. Pirch, W. Meiners, K. Wissenbach, R. Poprawe, Formation and reduction of hydrogen porosity during selective laser melting of AlSi10Mg, J. Mater. Process. Technol. 221 (2015) 112-120.

[2] N.T. Aboulkhair, N.M. Everitt, I. Ashcroft, C. Tuck, Reducing porosity in AlSi10Mg parts processed by selective laser melting, Addit. Manuf. 1-4 (2014) 77-86.

[3] W.E. King, H.D. Barth, V.M. Castillo, G.F. Gallegos, J.W. Gibbs, D.E. Hahn, C. Kamath, A.M. Rubenchik, Observation of keyhole-mode laser melting in laser powder-bed fusion additive manufacturing, J. Mater. Process. Technol. 214(12) (2014) 2915-2925.

[4] E. Louvis, P. Fox, C.J. Sutcliffe, Selective laser melting of aluminium components, J. Mater. Process. Technol. 211(2) (2011) 275-284.

[5] F. Haeckel, M. Meixlsperger, T. Burkert, Technological challenges for automotive series production in laser beam melting, Proceedings of the 28th annual international Solid Freeform Fabrication Symposium, Austin, Texas, 2017.

[6] M. Tang, P.C. Pistorius, Oxides, porosity and fatigue performance of AlSi10Mg parts produced by selective laser melting, Int. J. Fatigue 94(2) (2017) 192-201.

[7] N. Read, W. Wang, K. Essa, M.M. Attallah, Selective laser melting of AlSi10Mg alloy: process optimisation and mechanical properties development, Mater. Des. 65 (2015) 417-424.

[8] F. Trevisan, F. Calignano, M. Lorusso, J. Pakkanen, A. Aversa, E.P. Ambrosio, M. Lombardi, P. Fino, D. Manfredi, On the selective laser melting (SLM) of the AlSi10Mg alloy: process, microstructure, and mechanical properties, Materials 10(1) (2017) 76.

[9] N. Ellendt, F. Fabricius, A. Toenjes, PoreAnalyzer – an open-source framework for analysis and classification of defects in additive manufacturing, Appl. Sci. 11(13) (2021) 6086.

[10] A. Leis, R. Weber, T. Graf, Process windows for highly efficient laser-based powder bed fusion of AlSi10Mg with reduced pore formation. Materials 14(18) (2021) 5255.

[11] X. Cai, A.A. Malcolm, B.S. Wong, Z. Fan, Measurement and characterization of porosity in aluminium selective laser melting parts using X-ray CT. Virtual Phys. Prototyp. 10(4) (2015) 195-206.

[12] S. Romano, A. Abel, J. Gumpinger, A.D. Brandão, S. Beretta, Quality control of AlSi10Mg produced by SLM: metallography versus CT scans for critical defect size assessment. Addit. Manuf. 28 (2019) 394-405.

[13] C. Taute, H. Möller, A. du Plessis, M. Tshibalanganda, M. Leary, Characterization of additively manufactured AlSi10Mg cubes with different porosities. J. South Afr. Inst. Min. Metall. 121(4) (2021) 143-150.

[14] A. du Plessis, I. Yadroitsava, S.G. le Roux, I. Yadroitsev, J. Fieres, C. Reinhart, P. Rossouw, Prediction of mechanical performance of Ti6Al4V cast alloy based on microCT-based load simulation. J. Alloy Compd. 724 (2017) 267-274.

[15] N. Nudelis, P. Mayr, Defect-based analysis of the laser powder bed fusion process using X-ray data. Int. J. Adv. Manuf. Technol. 123 (2022) 3223-3232.

[16] M.R. Ogiela, L.C. Jain, Computational intelligence paradigms in advanced pattern classification, in: T. Sobol-Shikler, Inference of co-occuring classes: multi-class and multi-label classification, Springer, Berlin, Heidelberg, 2012.

[17] H. Demuth, M. Beale, Neural network toolbox. For Use with Matlab, The Mathworks. USA, 2004.

[18] N. Nudelis, P. Mayr, A novel classification method for pores in laser powder bed fusion, Metals 11(12) (2021) 1912.

[19] T. Agrawal, Hyperparameter optimization in machine learning, Apress, Berkeley, USA, 2021.

[20] G.W. Brier, Verification of forecasts expressed in terms of probability, Mon. Weather Rev. 78(1) (1950) 1-3.

[21] A.V. Joshi, Machine learning and artificial intelligence, Springer, Switzerland, 2020.

[22] M.F. Møller, A scaled conjugate gradient algorithm for fast supervised learning, Neural Netw. 6(4) (1993) 525-533.

[23] D. Nguyen, B. Widrow, Improving the learning speed of 2-layer neural networks by choosing initial values of the adaptive weights, IJCNN International Joint Conference on Neural Networks, San Diego, USA, 1990.

[24] N. Hasmuni, M. Ibrahim, A.A. Raus, M.S. Wahab, K. Kamarudin, Porosity effects of AlSi10Mg parts produced by selective laser melting, J. Eng. Mech. 5(4) (2018) 246-255.

[25] V.V. Kokareva, V.G. Smelov, A.V. Agapovichev, A.V. Sotov, V.S. Sufiiarov, Development of SLM quality system for gas turbines engines parts production, IOP Conf. Ser.: Mater. Sci. Eng. 441 (2018) 012024.

[26] S.L. Sing, W.Y. Yeong, Laser powder bed fusion for metal additive manufacturing: perspectives on recent developments, Virtual. Phys. Prototyp. 15(3) (2020) 359-370.

[27] D.D. Gu, W. Meiners, K. Wissenbach, R. Poprawe, Laser additive manufacturing of metallic components: materials, processes and mechanisms, Int. Mater. Rev. 57(3) (2012) 133-164.